8-2018

Immobilization of Gold Nanoparticles on Nitrided Carbon Fiber Ultramicroelectrodes by Direct Reduction

George Affadu-Danful
East Tennessee State University

Recommended Citation

Affadu-Danful, George, "Immobilization of Gold Nanoparticles on Nitrided Carbon Fiber Ultramicroelectrodes by Direct Reduction" (2018). *Electronic Theses and Dissertations.* Paper 3446. https://dc.etsu.edu/etd/3446

Immobilization of Gold Nanoparticles on Nitrided Carbon Fiber Ultramicroelectrodes by Direct Reduction

---

A thesis
presented to
the faculty of the Department of Chemistry
East Tennessee State University

In partial fulfillment
of the requirements for the degree
Master of Science in Chemistry

---

by
George Paa Kwesi Affadu-Danful
August 2018

Dr. Gregory W. Bishop, Chair
Dr. Dane W. Scott
Dr. Marina Roginskaya

Keywords: ultramicroelectrodes, gold nanoparticles, cyclic voltammetry, nitrided carbon fiber

ABSTRACT

Immobilization of Gold Nanoparticles on Nitrided Carbon Fiber Ultramicroelectrodes by Direct Reduction

by

George Paa Kwesi Affadu-Danful

Due to enhanced properties such as large surface area-to-volume ratio, metal nanoparticles are often employed as catalysts for various applications. However, most studies involving nanoparticle catalysts have been conducted on collections of particles rather than single nanoparticles. Results obtained for ensemble systems can be difficult to interpret due to variations in particle loading and interparticle distance, which are often challenging to control and characterize. In this study, two immobilization strategies for incorporating gold nanoparticles (AuNPs) on carbon fiber ultramicroelectrodes (UMEs) were compared with the goal of extending these techniques to nanoelectrodes for studies of single AuNPs. Both layer-by-layer deposition of AuNPs on natural carbon fiber UMEs and direct reduction of AuNPs on nitrided carbon fiber UMEs were explored. Although both methods proved feasible, the direct reduction method seemed to be more effective and should better enable direct comparisons of bare and capped AuNPs.

DEDICATION

This work is dedicated to my mother Leticia Adjei.

ACKNOWLEDGMENTS

I thank God Almighty for His guidance and divine protection upon my life from infancy till now. I am forever grateful.

I am very indebted to my research advisor Dr. Gregory W. Bishop for his honest support, assistance and guidance through my period of study at ETSU. He played a key role during my phase of professional training and I am highly appreciative to him for all he taught me and all I have learned from him. I also thank my thesis committee faculty Dr. Marina Roginskaya and Dr. Dane Scott for their expertise, support and also accepting to be on my thesis committee. I am also thankful to all chemistry department faculty and staff for their assistance during my period of study at ETSU.

I am thankful to my parents Mr. Daniel Affadu, Mrs. Margaret Affadu, Mr. Francis Baidoo, Mrs. Leticia Baidoo and my entire family for their love and support throughout my life. I appreciate the support from Apostle Dr. Arnold Nyarambi and Pastor Dumisa Nyarambi. I thank my friends; Evans Addo, Millicent Arthur, Selasi Dzansi, Emmanuel Osei-Ansah, Obed Koomson, Edward Acheampong, Augustin Oppong, and all my friends. I want to appreciate my lab partner Theophilus Neequaye for being a great person to work with and also all students in Dr. Bishop’s research lab.

I also acknowledge the American Chemical Society Petroleum Research Fund (Award # 58123 – UN15) for funding this work and also Dr. Xu Feng and the Surface Analysis Laboratory at Virginia Tech for the XPS analysis.

TABLE OF CONTENTS

LIST OF TABLES

LIST OF FIGURES

LIST OF ABBREVIATIONS

AFM – Atomic Force Microscopy
AuNP – Gold Nanoparticle
CV – Cyclic Voltammetric
EDX - Energy-Dispersive X-ray Spectroscopy
$FcCH_2OH$ – Ferrocenemethanol
GSH-AuNPs – Glutathione-Capped Gold Nanoparticles
HER – Hydrogen Evolution Reaction
I.D – Internal Diameter
LbL – Layer-by-Layer
LSPR – Localized Surface Plasmon Resonance
MNP – Metal Nanoparticle
NHE – Normal Hydrogen Electrode
O.D – Outer Diameter
ORR – Oxygen Reduction Reaction
PAN - Polyacrylonitrile
PDDA - Poly(diallyldimethylammonium)
SCE – Saturated Calomel Electrode
SECM – Scanning Electrochemical Microscopy
SPR – Surface Plasmon Resonance
TEM- Transmission Electron Microscopy
UME – Ultramicroelectrode
XPS – X-ray Photoelectron Spectroscopy

CHAPTER 1

INTRODUCTION

Metal Nanoparticles

Nanoparticles are particles with sizes less than 100 nm.[1] Due to their much larger surface area-to-volume ratios compared to bulk materials, particles in this size range can exhibit different properties from bulk materials of similar composition. Nanoparticles exhibit unique electronic and optical properties[2] which find relevant applications in areas such as catalysis[3,4], sensors and spectroscopy.[5-7] As a result, nanoparticles have gained much attention in various areas of research.

Metal nanoparticles (MNP) have been particularly widely studied due to their interesting optical properties[8] and abilities to promote reactions that do not typically proceed at bulk surfaces under normal conditions[9]. Metal nanoparticles are typically produced in suspensions from metal ion precursors, reducing agents, and organic ligands called capping agents[10]. Based on the intended application, the size of MNPs can be controlled to achieve specific properties and functions. When synthesized in solution, metal nanoparticles show fast dispersion rate and therefore tend to agglomerate.[11] Organic ligands known as capping agents bind to surface sites and help reduce agglomeration rate, fix nanoparticle size, and promote monodispersity.[11]

While there have been extensive studies focused on examining the relationship between nanoparticle size, shape, composition and catalytic activity,[9] most of these studies involving nanoparticle catalysts have been conducted on collections, ensembles, or arrays of particles. For example, Shao[12] and coworkers studied electrocatalysis of the oxygen reduction reaction (ORR) in $HClO_4$ with ensembles of platinum nanoparticles ranging from 1-5 nm in diameter supported on carbon black (Ketjen Black). The size of the platinum nanoparticles was controlled by a layer-by-layer growth method by means of copper underpotential deposition on 1.3 nm platinum nanoparticle seeds (10% by weight) supported on Ketjen Black followed by spontaneous displacement of copper with platinum using Pt(IV) at the open circuit potential.[13] Particles within the size range of 1.3 to 2.2 nm showed increased mass activity towards ORR by about 4-fold. However, a slow increase in mass activity towards ORR was observed as the particle size increased from 2.2 nm. Also, Misty et. al[14] demonstrated size dependency on catalytic activity of gold nanoparticles (AuNP) towards CO_2 reduction in $KHCO_3$. AuNP deposited on a glassy carbon electrode were synthesized by inverse micelle encapsulation[15] followed ligand removal using O_2 plasma treatment. From linear sweep voltammetric experiments, they reported a significant increase in current density (which is proportional to catalytic activity) alongside decreasing Faradaic selectivity towards CO as nanoparticle size decreased.

Though most measurements of electrocatalytic activity of nanoparticles have been obtained using multiple nanoparticles dispersed on solid surfaces, results from these systems are subject to effects of particle loading and interparticle distance (Figure 1).[16-20] Kumar and Zou[18] reported that, as interparticle distance increases, catalytic activity decreases. In their study, they synthesized gold nanoparticle (AuNP) arrays with uniform interparticle spacing through use of argon plasma treated polystrene-b-poly(2-vinylpyridine) as a template. Increasing interparticle distances between 28 and 80 nm showed a significant increase in half-wave potentials for CO oxidation, which indicated decreasing electrocatalytic activity.[19]

Also, Taylor and coworkers[20] studied nanoparticle loading effects on the catalytic activity of platinum nanoparticles towards the ORR. Platinum nanoparticles with size range between 3.4 and 5.5 were deposited on carbon electrode by thermal induction chemical deposition. An increase in platinum loading on carbon changed the morphology of the particles. Platinum agglomerates and nanoparticles were characterized by the appearance of low and high potentials for CO oxidation, respectively. Low platinum loadings exhibited higher activity than high platinum loadings towards ORR. Conversely, unlike Taylor and coworkers,[20] Higuchi et al.[16] reported that nanoparticle loading showed no dependence on catalytic activity. The area-specific activity of platinum nanoparticles loaded on carbon black between 19.2 and 63.2 wt% had no influence on catalytic activity toward the ORR. Cyclic voltammetric experiments conducted at working disk electrode in deaerated $HClO_4$ revealed that, potentials relating to area specific ORR activity stayed constant regardless of the platinum loading level between 19.2 to 63.2%.

Interparticle distance and particle loading of ensembles are often challenging or impossible to control and characterize. These complications can make it problematic to compare results obtained for different electrocatalytic systems for optimization purposes, even for the same reaction. Single nanoparticle studies[21-24] should help uncover direct relationships between nanoparticle size, surface properties, and catalytic activity through measurements that are unobscured by complex factors such as interparticle distance and particle loading. Results from single nanoparticle experiments may therefore enhance understanding of the nanoparticle structure-function relationship and aid in the development of better nanoparticle-based catalysts.

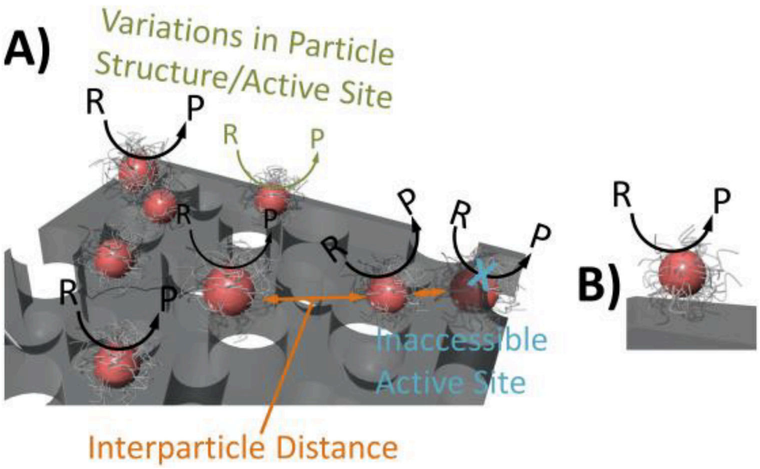

Figure 1: Illustrated representations of nanoparticle ensemble and single nanoparticle measurements. Catalytic conversion of reactant R to product P is promoted on a nanoparticle ensemble (A) and a single nanoparticle (B).

Studying Electrocatalytic Properties of Single Nanoparticles using Electrochemical Techniques

Studies of the electrocatalytic properties of single nanoparticles can be achieved by two major methods: 1) by nanoparticle impact techniques, or 2) the use of nanometer-sized electrodes as platforms for depositing a single nanoparticle so that electrochemical behavior of the particle can be explored.[25-29]

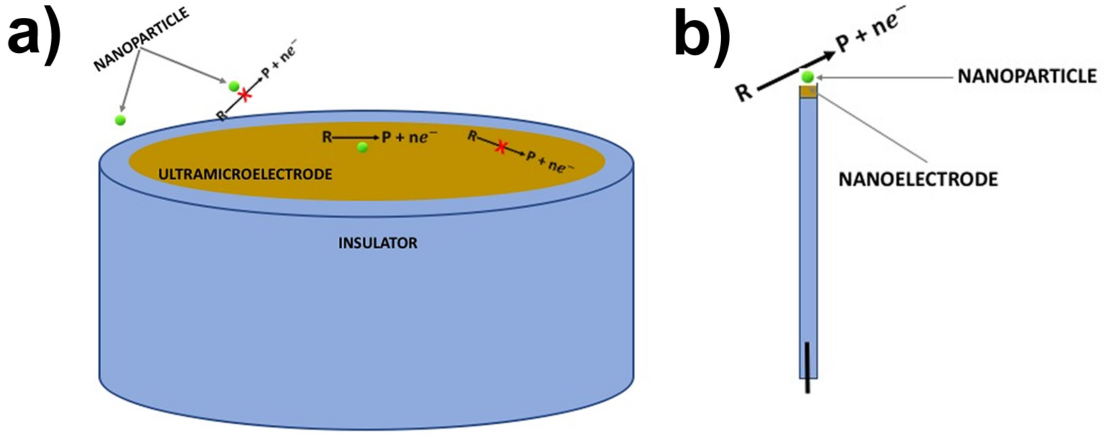

Figure 2: Schematic representation of single nanoparticle electrochemical measurement techniques. In nanoparticle impact methods (a), the oxidation of reactant R to product P only occurs if the nanoparticle is in contact with the electrode surface which is held at a sufficient potential. In single nanoparticle immobilization (b), the electrode is small enough to accommodate attachment of only one nanoparticle. The oxidation of reactant R to product P can be evaluated using voltammetry or other electrochemical methods.

Nanoparticle Impact Studies

Nanoparticle impact studies involve holding an ultramicroelectrode (UME, electrode with size <25 μm) at a potential where no electrochemical reaction occurs at the electrode surface, but one that is sufficient to promote direct or electrocatalytic reactions at nanoparticles. Nanoparticles in solution will produce transient changes in current as electron transfer occurs when they collide with or stick on the electrode surface.[10,21,30,31] The magnitude, shape, and frequency of the current fluctuations are related to particle size, concentration, and reaction kinetics.[32]

Xiao and Bard were pioneers in developing a method that can be used to study single nanoparticles through nanoparticle collision events.[27] Nanoparticles can act as catalyst[3,4] for certain reactions while bare UMEs do not. In their experiments, step-like events that appeared in the current-time trace correlated to collisions and adsorption of platinum nanoparticles onto an UME held at a constant potential since the platinum nanoparticles were capable of acting as electrocatalysts while the UME was not.[33] When a nanoparticle collides an UME surface, the open circuit potential of the UME also changes, which provides another method that can be used to measure single nanoparticle electrocatalysts. Stevenson et.al used a mercury modified platinum UME to detect platinum nanoparticles[33] by measuring changes in open-circuit potential that result when platinum nanoparticles strike the electrode surface.

Single Nanoparticle Immobilization on Nanoelectrode

Studying electrochemical and electrocatalytic properties at the single nanoparticle level through immobilization of an individual nanoparticle on an electrode requires the use of an electrode with size similar to that of the particle.[25] These nanoelectrodes can be fabricated by various means which include insulating a metal wire or carbon fiber in a glass capillary by the use of micropipette puller[34-36] and chemical vapor deposition of materials such as metals or pyrolyzed carbon into glass nanopipettes.[37,38]

In addition to nanoelectrode fabrication, isolation of an individual nanoparticle on the electrode surface and verification of single particle modification are also critical steps in completing these types of studies. Adsorption or attachment of nanoparticles can be achieved through covalent bonding[37] or electrostatic[39] interactions with chemically modified nanoelectrode surfaces (Table 1). In some cases, metal ions can also be reduced directly onto the bare nanoelectrode surface without any chemical modification to produce a single nanoparticle of interest.[40]

Sun et al. immobilized a gold nanoparticle on a 42 nm platinum electrode by spontaneous deposition of Au from a 1 % $HAuCl_4$ solution.[40] The presence of a single gold nanoparticle on the electrode surface was confirmed by scanning electron microscopy, energy-dispersive X-ray spectroscopy (EDX) and cyclic voltammetry (CV).[32] CVs of the Pt nanoelectrode with immobilized AuNP in 0.5 M H_2SO_4 exhibited a small cathodic peak at ~600 mV, which corresponds to Au oxide stripping. The position of the oxide stripping peak was dependent on nanoparticle size with smaller particles possessing more negative peak potentials.

In a separate study, Zhang et al. attached single gold nanoparticles (10-30 nm) from a colloidal suspension onto ~10 nm platinum electrodes modified with an amine silane.[25] Electrocatalysis of the oxygen reduction reaction (ORR) at single nanoparticles was found to be affected by nanoparticle size. A 24 nm AuNP immobilized on a Pt nanoelectrode exhibited ORR half-wave potentials at more positive values and produced larger currents than 18 and 14 nm AuNPs, indicating increasing electrocatalytic activity with increasing nanoparticle diameter in this size regime.

Mirkin et al. attached single citrate-capped AuNPs onto a carbon nanoelectrodes by three different methods: direct attachment, electrostatic adsorption and covalent binding.[26] Electrostatic adsorption and covalent binding was accomplished by modifying the carbon surface with a multilayer polyphenylene film generated by electrochemical reduction of an aryl diazonium salt. The direct attachment was carried out by adsorption of an AuNP onto the electrode by immersing the electrode in an AuNP solution for 1.5 to 2 hours.

By comparing voltammograms of the hydrogen evolution (HER) reaction from $HClO_4$, AuNP modified electrodes showed enhanced catalytic activity observed by significant increase in current compared to bare electrodes. However, HER at AuNP modified electrodes prepared by direct attachment occurred at more positive potentials compared to polyphenylene film modified AuNP electrodes. The significant difference observed might be due to the polyphenylene film acting as an insulator hence inhibiting electron transfer between the carbon surface and the AuNP.[26] Direct attachment of AuNP to electrode surface seems to be a more effective method compared to electrodes modified with AuNP via films. However, according to Mirkin et al., the mechanism of direct attachment of a single NP to the bare carbon surface is not clear, and the electrochemical response for an NP immobilized this way was only stable over the course of a few hours.[26]

Table 1: Selected nanoparticle immobilization strategies on nanoelectrodes

Authors (Year)	Electrode Type, Radius (nm)	Nanoparticle Type, Radius (nm)	Particle Immobilization	Reaction Studied
Zhang et al. (2010) [25]	Pt (10)	Au (20-60)	Amine silane linker	ORR[a]
Mirkin et al. (2015) [37]	C (2-16)	Au (<40)	Direct Adsorption, Electrostatic Adsorption, Covalent binding	HER[b]
Sun et al. (2013)[40]	Pt (42)	Au (NP)[c]	Spontaneous deposition	Reduction of gold oxide
Lakbub et al. (2011)[41]	Pt (8)	Au (3.3-4.7)	Electrostatic Adsorption	Reduction of gold oxide
Clausmeyer et. al (2015)[42]	C (<100)	$Ni(OH)_2$ (20-500)	Electrodeposition	ORR[a]

[a]Oxygen Reduction Reaction
[b]Hydrogen Evolution Reaction
[c]Not Reported

Research Objectives

Studies of electrocatalysis at the single nanoparticle level are not subject to complications associated with ensemble studies. Complication in ensemble studies surfaces from averaging effects and variations due to factors like interparticle distance that are inherent in typical investigations of electrocatalytic properties based on collections of particles that are distributed on conductive supports. As such, studies involving individual nanoparticles should provide an excellent platform for characterizing the relationship between nanoparticle structure and catalytic function that is crucial to developing and optimizing advanced electrocatalysts for important energy and industrial applications.

In the present study, strategies for immobilizing bare and capped gold nanoparticles on carbon ultramicroelectrodes were investigated to determine their feasibility in enabling measurement of electrochemical and electrocatalytic properties of single nanoparticles. Glutathione-capped gold nanoparticles were attached to carbon ultramicroelectrodes through a layer-by-layer electrostatic adsorption process that has proven effective on bulk pyrolytic graphite and screen-printed carbon macroelectrodes.[51,55] To immobilize bare gold particles, carbon electrodes were modified with surface nitrogen groups via a recently reported nitriding procedure[43] that was used to prepare AuNP composite materials from various carbon supports, including carbon blacks, activated carbons and mesoporous carbons. In the studies presented here direct reduction of gold (III) chloride preferentially at surface nitrogen groups on nitrided carbon fiber electrodes also proved to be a feasible way of immobilizing bare AuNPs onto carbon fiber UMEs.

While both the layer-by-layer and nitriding immobilization strategies have shown to be reasonable strategies for attachment of AuNPs on UMEs, direct reduction of bare AuNPs on nitrided carbon fiber UMEs seems to be a more effective way of studying electrochemical properties of single nanoparticles, since it avoids complexities associated with PDDA films and should allow comparison of bare and capped nanoparticles.[44]

CHAPTER 2

EXPERIMENTAL

Materials

All chemicals were used as received from the manufacturer. Ferrocenemethanol ($FcCH_2OH$), potassium chloride, and an aqueous solution of 20% (w/w) PDDA (average molecular weight range 200,000-350,000) were obtained from Sigma-Aldrich. Urea, L-glutathione and tetrachloroaurate (III) trihydrate were supplied by Alfa Aesar. Silver paste was purchased from Beantown Chemical (Hudson, NH). Sodium borohydride was purchased from Fisher Scientific. Quartz and borosilicate glass capillaries were purchased from Sutter Instruments Company. Nichrome wire was purchased from Parr Instrument Company. Carbon fiber was obtained from Goodfellow Cambridge Limited. All aqueous solutions were prepared with 18.2 MΩ·cm ultrapure water, made by passing deionized water through a Millipore Synergy purifier.

Nitriding of Carbon Fiber

Commercially available carbon fibers with diameter of 7 µm and length of ~10 cm were modified with nitrogen-containing functional groups through the process of "soft nitriding", which was completed by annealing the fiber in urea.[43,44] The carbon fiber was mixed with urea and placed in an oven at 150 ^{o}C for 2 hours and then 250 ^{o}C for another 2 hours. The annealed carbon fiber was carefully washed with ethanol followed by ultrapure water. The washed nitrided carbon fiber was then kept in the oven to dry to make it ready for electrode fabrication.

X-Ray Photoelectron Spectroscopy

X-ray photoelectron spectroscopy analysis was carried out by Dr. Xu Feng at the Surface Analysis Laboratory at Virginia Tech using a PHI VersaProbe III. Collections of the fibers were taped to a sample holder and introduced to the instrument.[45] Spectra were acquired using monochromatic Al K-alpha X-ray source (1486.6 eV) at 100 W over 1400 × 100 µm area at 45° angle. All binding energies were referenced with respect to adventitious C-C at 284.8 eV. Chemical states of elements were assigned based on the PHI and NIST XPS Databases.

Fabrication of Carbon Fiber Ultramicroelectrode

Untreated carbon fiber and nitrided carbon fiber ultramicroelectrodes were fabricated by the laser-assisted pulling method using a Sutter Instruments P2000 laser-based micropipette puller. A single bare or nitrided carbon fiber was inserted into a borosilicate glass capillary tube (1.0 mm OD, 0.5 mm ID, 10 cm length) via vacuum aspiration. The presence of carbon fiber in borosilicate glass capillary was confirmed with a Nikon microscope interfaced with a Pixelink camera connected to a computer. The glass capillary was then clamped into the puller arms of the pipette puller, and both open ends were connected to a vacuum pump via Tygon tubing.

Typical parameters applied to the programmable pipette puller were Heat 450, Filament 1, Velocity 15, Delay 80, Pull 0. All the parameters used on the pipette puller are dimensionless and therefore do not represent actual temperature or velocity.[46,47] The program was repeated twice with puller stop bars in place to avoid the formation of electrodes with undesirably long, tapered ends that proved to be difficult to work with due to their fragility. The capillary tube was pulled under vacuum in order to create a seal between the carbon fiber and glass upon application of laser heat. After the capillary tube was split into two with carbon fiber sealed in the ends exposed to the laser heat, wires were connected to each fiber through each unsealed end in order to provide electrical connections necessary for interfacing the electrodes with electrochemical instruments. Each glass capillary with sealed fiber was carefully polished on 800 grit abrasive paper to expose a disk-shaped portion of carbon that serves as an electrode. Manual polishing of electrodes requires extreme care and control due to the fragile nature of these electrodes.

Characterization of Carbon Fiber Electrodes

Electrode sizes were determined using cyclic voltammetry (CV).[48] A two-electrode system was used for the measurements with the carbon fiber electrode functioning as the working electrode and an Ag/AgCl electrode (Bioanalytical Systems) as the reference/counter electrode. The electrodes were place in a solution of 0.5 mM $FcCH_2OH$ in 0.1 M potassium chloride, and CVs were taking using a Bioanalytical Systems Epsilon electrochemical workstation operating in potentiostatic mode.

Working electrodes with dimensions <25 µm exhibit sigmoidal voltammetric responses towards Faradaic electrochemical reactions involving common redox probes[49] like $FcCH_2OH$. The steady-state limiting current (i_{ss}) is related to the size of the electrode, and the electrode radius can be estimated through use of equation 1. [1,22,60]

$$i_{ss} = 4nFDrc^* \qquad (1)$$

where n is the number of electrons transferred for the redox reaction per mole of reactant, F is Faraday's constant, r is the electrode radius in cm, and D and c^* are the diffusion coefficient (in cm^2/s) and bulk concentration of reactant (in mol/cm^3), respectively. The diffusion coefficient of $FcCH_2OH$ is 7.80×10^{-6} $cm^2\,s^{-1}$.[10,49,50]

Synthesis of Glutathione-Capped Gold Nanoparticles

Glutathione-capped gold nanoparticles (GSH-AuNPs) were synthesized using a previously reported procedure and subsequently employed to modify carbon fiber electrodes through a layer-by-layer electrostatic adsorption technique.[51,55] Hydrogen tetrachloroaurate ($HAuCl_4 \cdot 3H_2O$) and L-glutathione were added to a small vial and dissolved in a 14.4% (v/v) acetic acid in methanol mixture using a stir bar and magnetic stirrer. The resulting solution was bright yellow in color. 1.5 mL of 7.9 mM sodium borohydride was added dropwise into the gold mixture with continuous stirring. The color of the mixture immediately changed from yellow to brown. The mixture was stirred rapidly for 2 hours, resulting in a suspension of glutathione-capped gold nanoparticles (GSH-AuNPs).

The GSH-AuNPs suspension was divided into two 50 kDa MW cut-off filter centrifuge tubes. The suspensions were centrifuged at 2150xg for 8 min using a VWR Clinical 100 centrifuge to remove smaller particles and unreacted reagents. Particles of sufficient size were collected in the upper filter insert while the liquid in the bottom of the centrifuge tube was removed and disposed. The GSH-AuNPs were suspended in ultrapure water and centrifuged. This washing process was repeated three more times. The GSH-AuNPs were then washed with 20 mM HEPES buffer(pH=8) in the same manner five times. The GSH-AuNP were finally resuspended in 1.5 mL HEPES buffer and stored in microcentrifuge tubes at 4 ^{o}C.[51,52]

Characterization of GSH-AuNPs

UV-Vis spectroscopy was used to estimate the size of the GSH-AuNPs.[53] From the UV-Vis spectrum (Figure 3) an absorbance peak of 512 nm (λ_{SPR}) was observed as a result of surface plasmon resonance[54] corresponding to particles with diameter smaller than 30 nm as reported in literature.[53] The ratio of absorbance at 512 nm to absorbance at 450 nm (A_{SPR}/A_{450}) was used to estimate the size of the GSH-AuNP particles.[53] This was based on the fact that the absorbance at the surface plasmon resonance is known to decrease relative the absorbance occurring at other wavelengths in a way that is related to particle size.[53] The size of the particle was estimated to be 4 nm. The size of the particles agrees with particles synthesized using the same procedure and characterized by UV-Vis spectroscopy and transmission electron microscope (TEM) as reported in literature.[55]

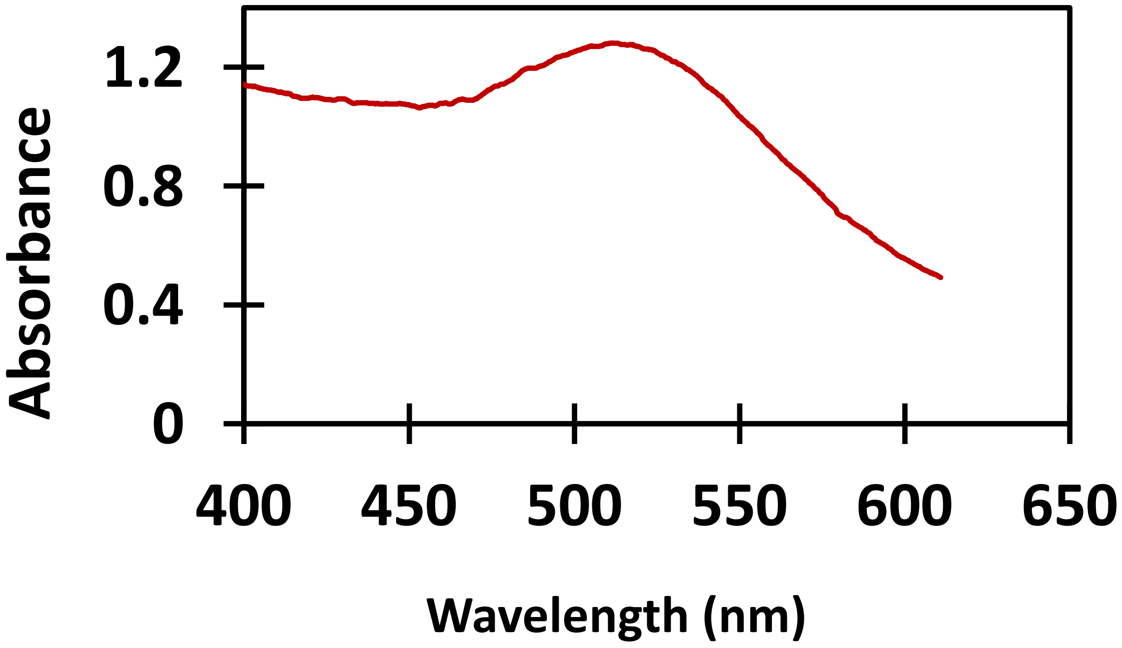

Figure 3: Absorption spectrum of GSH-AuNPs in 20 mM HEPES buffer (pH 8.0). Characteristic absorption peak is at 512 nm.

Layer-by-Layer Modification of Ultramicroelectrode with GSH-AuNPs

To attach the GSH-AuNPs to the carbon fiber UME surface, a layer-by-layer (LbL) electrostatic adsorption strategy was employed.[51] The carbon fiber UME was first conditioned by a linear voltammetric sweep from -1400 mV to + 2000 mV vs. Ag/AgCl reference electrode in

0.5 M H_2SO_4 [51]. The electrode was then rinsed with water and allowed to dry. The electrode was carefully placed in a solution of poly(diallyldimethylammonium chloride) (PDDA) (2 mg/mL in 0.05 M NaCl) for 2 hours to enable electrostatic adsorption of the PDDA polycation. After drying, the electrode was then placed into GSH-AuNPs suspension for another 2 hours so that the GSH-AuNPs could be immobilized on the PDDA layer through interaction of the negatively charged surface carboxylate groups with the positive cation. Then the electrode was finally rinsed with ultrapure water and dried to remove loosely adsorbed GSH-AuNPs.[51,55]

Modification of Untreated and Nitrided Carbon Fiber UMEs with Uncapped Gold Nanoparticles

Natural (untreated) and nitrided carbon fiber UMEs were carefully suspended in a solution of 25 μM $HAuCl_4 \cdot 3H_2O$ with the tip of the electrode exposed to the gold chloride solution. Gold nanoparticles were synthesized on the electrode surface by direct reduction.[56] A 26 mM sodium borohydride was added dropwise for a total of 0.2 mL over the course of 10 min while the gold solution was sonicated. Sonication was continued for 2 hours. Finally, the electrode was removed from the gold mixture, rinsed with water and dried.

CHAPTER 3

RESULTS AND DISCUSSION

Electrochemical Behavior of Carbon Fiber UMEs Modified with GSH-AuNPs by Layer-by-Layer Electrostatic Adsorption

Natural (unmodified) carbon fiber electrodes prepared by laser-assisted pipette pulling were characterized by CV (Figure 4). The $FcCH_2OH/FcCH_2OH^+$ redox couple exhibited sigmoidal current-potential relationship indicative of disc-shaped electrodes with low micrometer to sub- micrometer size. Electrode size estimated from the CV steady-state limiting current (Equation 1)[1,22,57] indicated that the effective radius of the carbon fiber electrode was 2 μm.

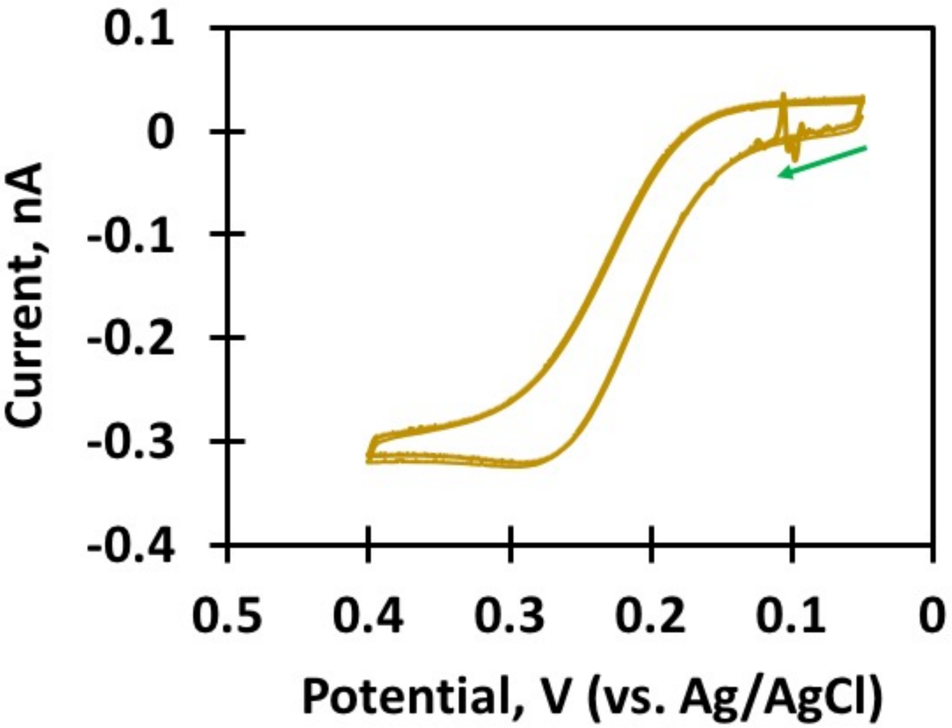

Figure 4: Representative CV of 0.50 mM ferrocene methanol in 0.10M KCl with natural carbon fiber UME. Arrow indicates direction of scan. Scan rate is 10 mV/s.

Natural carbon fiber UMEs were modified with gold nanoparticles through a simple layer-by-layer technique using cationic PDDA to electrostatically adsorb GSH-AuNPs, which are negatively charged due to surface carboxylate groups.[51,55] Successful modification of the electrode surface with AuNPs was confirmed by electrochemical measurements (Figure 5). CVs of GSH-AuNP/PDDA-modified carbon fiber UMEs in 0.50 M H_2SO_4 exhibited an anodic wave at +1.25 V and a cathodic peak at +0.83 V vs. Ag/AgCl, corresponding to oxidation of gold and subsequent reduction[58,60] of gold oxide, respectively.

It has been reported that the positions of peaks associated with redox processes of AuNPs are dependent on nanoparticle size.[9,60] Alexeyeva and Tammaveski[58] modified a glassy carbon electrode with 15 (± 3) nm AuNPs oxygen reduction. AuNPs were electrostatically adsorbed to the glassy carbon surface via a layer-by-layer attachment strategy using a PDDA-multi-wall carbon nanotube composite to study. CVs in H_2SO_4 of the AuNP-modified electrode showed anodic and cathodic peaks at +1.15 and +0.88 V vs SCE, respectively. Also, Zhang and coworkers[60] used a 5 μm gold UME modified with an AuNP network to sense single-cell exocytotic dopamine release AuNPs were immobilized (~8 nm in diameter) using a on sol-gel derived from (3-mercaptopropyl) trimethoxysilane that was deposited on the electrode surface. CVs of the AuNP network electrode in H_2SO_4 showed a reduction peak at +0.8 V vs Ag/AgCl which is comparable with what is reported in this work.

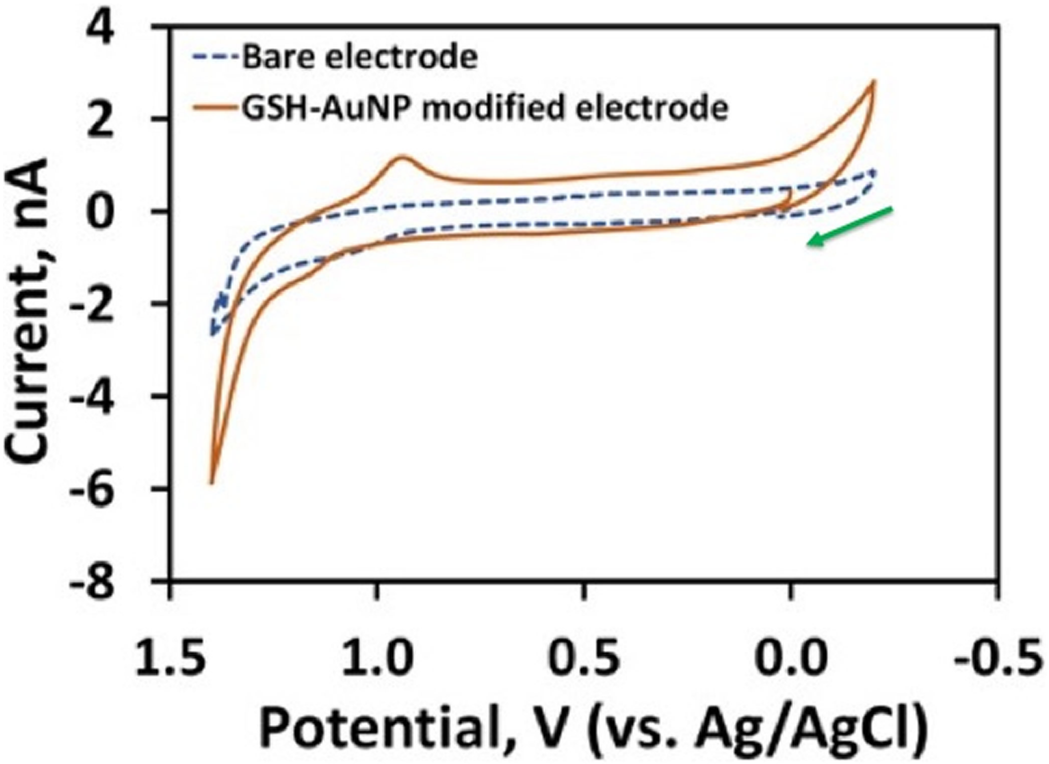

Figure 5: Representative CV responses of GSH-AuNP-modified carbon fiber UME taken in 0.50 M H_2SO_4. Arrow indicates direction of forward scan. Scan rate is 100 mV/s.

The charge related to the gold oxide reduction peak for the GSH-AuNP/PDDA- modified carbon fiber UME at +0.83V can be used to determine the surface area corresponding to the AuNP coverage.[58,60] For a monolayer of gold, the integration of this reduction peak results in a charge of 400 μC cm^{-2}.[58-60] In this case, the charge associated with the nanoparticle coverage was found to be 73.8 pC. This corresponds to an active gold surface area of 18.45 μm^2. The estimated AuNP electroactive surface area for electrostatically adsorbed particles on the carbon fiber UME surface is approximately six times larger than the geometric surface area of the carbon fiber UME.

Assuming nanoparticles are spherical, and particle diameter of 4 nm based on the ratio of absorbance at 512 nm to absorbance at 450 nm (A_{SPR}/A_{450}) from the UV-Vis spectrum (Figure 3), the surface area of a spherical gold nanoparticle can be estimated to be about 50 nm^2. With active area of coverage and area of a single gold nanoparticle known, approximately 366,000 capped gold nanoparticles were estimated to be immobilized onto the GSH-AuNP/PDDA-modified carbon fiber. [9,59] For comparison, Zhang and coworkers[60] reported in their study with AuNP network electrodes that, approximately 1.4 million AuNPs were immobilized onto the 5 µm UME.

Direct Reduction of Bare Gold Nanoparticles onto Untreated Carbon Fiber UME Surface

In order to compare electrochemical behaviors of bare and capped gold nanoparticles, direct reduction of $HAuCl_4 \cdot 3H_2O$ using sodium borohydride as a reducing agent was explored as a method for depositing ligand-free (bare) AuNPs onto the natural (untreated) carbon fiber electrode surface with the size of 6 µm (Figure 6).[1,22]

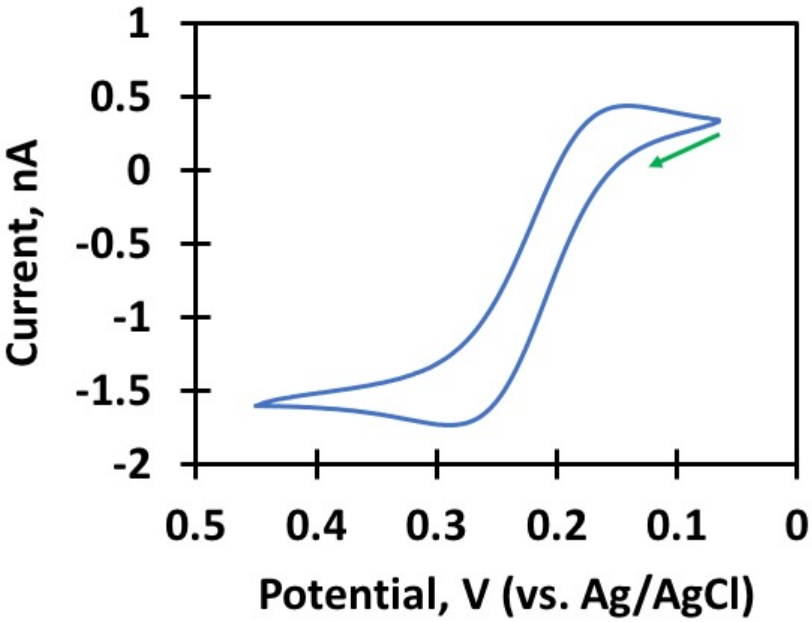

Figure 6: Representative CV of 0.50mM ferrocene methanol in 0.10M KCl with bare carbon fiber UME. Arrow indicates direction of scan. Scan rate of 25 mV/s.

After carrying out the deposition step for about 24 hours, it was shown that the gold deposition onto the untreated carbon fiber electrode surface was unsuccessful. The characteristic anodic and cathodic peaks associated with the oxidation and reduction of gold were not observed (Figure 7), indicating that modification of the electrode surface with bare gold particles was unsuccessful.

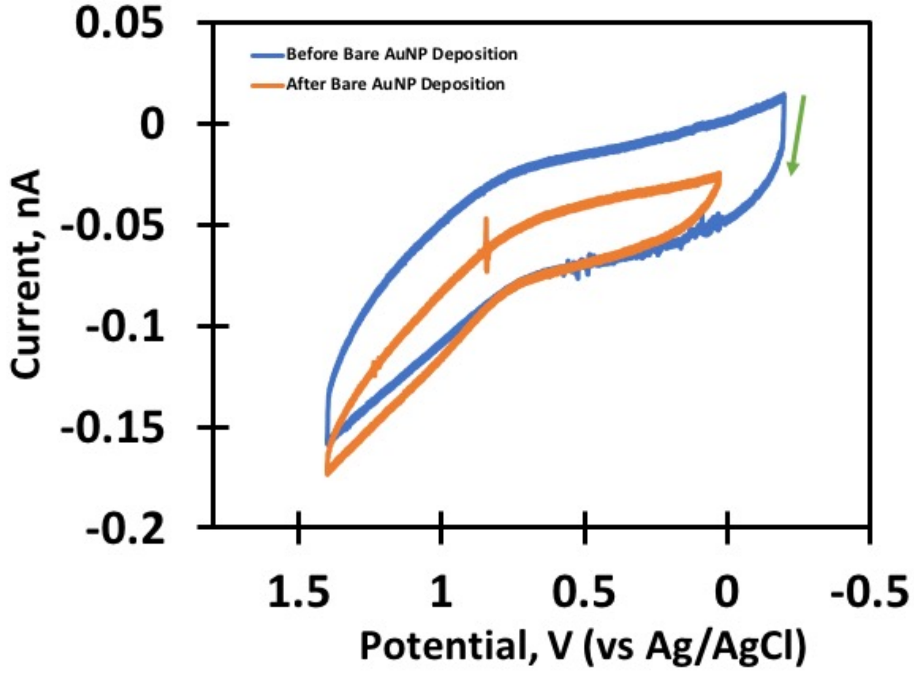

Figure 7: Representative CV responses of natural carbon fiber UME taken in 0.50 M H_2SO_4 showing unsuccessful attachment of AuNP after deposition strategy. Arrow indicates direction of scan. Scan rate is 25 mV/s.

Characterization of Nitrided Carbon Fiber Electrodes

Since modification of carbon fiber UMEs with bare AuNPs was unsuccessful, carbon fiber electrodes were modified with surface nitrogen groups through a “soft nitriding” method that was recently shown to promote deposition of highly electrocatalytic bare AuNPs on various carbon supports, including carbon blacks, activated carbons, and mesoporous carbons. [43,44]

Determining Surface Nitrogen Content Before and After Nitriding of Carbon Fiber by XPS

Elemental composition of carbon fibers before and after nitriding was ascertained by XPS (Figure 8). Unlike carbon supports employed in previous soft nitriding experiments,[43,44] carbon fibers used here featured surface nitrogen groups before modification. Prior to nitriding, carbon fibers exhibited XPS peaks corresponding to C1s (284.8 eV), N1s (400 eV), and O1s (531.3 eV), with relative abundances of 79%, 4%, and 17%, respectively (Table 2). The nitrogen present in the carbon fiber before the nitriding process is attributed to the industrial synthesis of the carbon fiber.[61]

The carbon fibers used in these studies were commercially synthesized from polyacrylonitrile (PAN). Polymerization is followed by a carbonization step which aids in the removal of oxygen, hydrogen, nitrogen and other elements aside carbon. The graphitization step is also carried out to further remove non-carbon compounds. However, the graphitization process is not one 100% efficient and hence some nitrogen groups remain on commercially available carbon fibers.[61] Through XPS analysis Viswanathan and coworkers reported that carbon fibers derived from PAN often exhibit surface nitrogens.[62] Smiley and Delgass[63] reported that untreated Cellion 6000 carbon fibers, which are also manufactured from PAN, contained 3% nitrogen on the surface as measured by XPS.

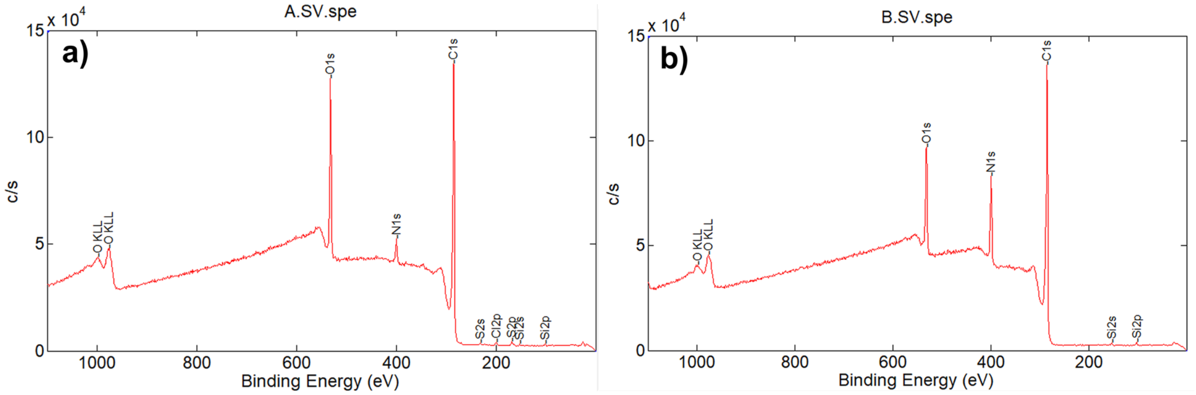

Figure 8: XPS spectra of carbon fiber (a) before and (b) after nitriding

Table 2: Percent composition of fiber samples

Fiber Sample	**C**	**N**	**O**
Natural	78.84 (± 1.87)	4.08 (± 0.07)	17.08 (± 1.80)
Nitrided	74.02 (± 2.08)	13.94 (± 0.23)	12.04 (± 1.85)

Nitriding led to an increase in intensity of the N1s peak (Figure 8) indicating successful modification of the fiber surface with nitrogen groups. The increase in surface nitrogen content corresponded to a ~3.5x larger atomic concentration of nitrogen compared to carbon fibers that were not nitrided (Table 1), and also coincided with a significant decrease in oxygen atomic concentration from 17% for the natural fiber to 12% for the nitrided carbon fiber. This decrease in atomic oxygen concentration suggests that nitriding occurs preferentially at oxygen-containing surface sites, which is consistent with previously reported literature.[62]

Type of Nitrogen Groups Present on Natural and Nitrided Carbon Fibers

Deconvolution of the XPS N1s peaks was completed in order to determine the types of nitrogen species present in natural and nitrided carbon fibers. The natural carbon fiber N1s XPS spectrum matched well with a 3-peak model consisting of pyridinic (398.43 eV), amine/amide (399.96 eV), and ammonium (402.13 eV) nitrogens (Figure 9). The majority of the nitrogen atoms on the natural carbon fiber (77.45%) were found to be from amine/amide groups.

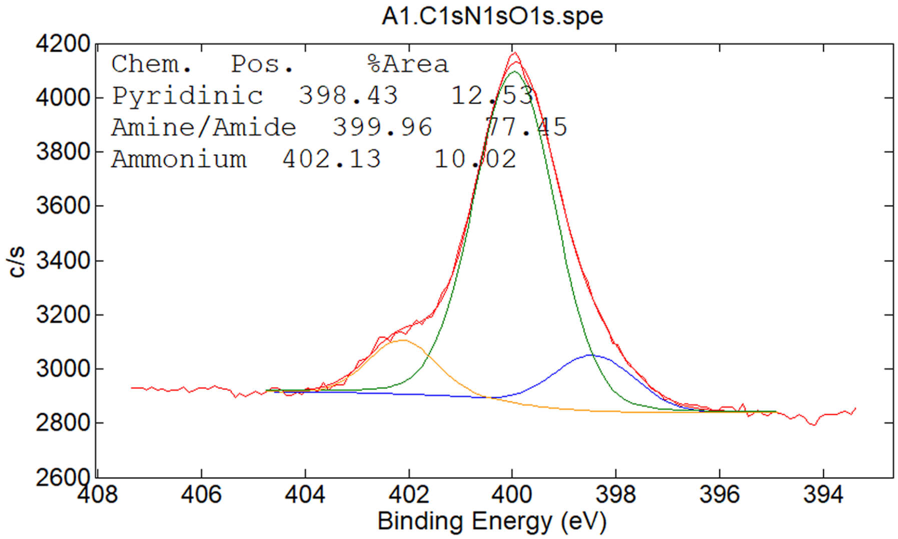

Figure 9: XPS spectra of types of nitrogen compounds present before nitriding carbon fiber

Deconvolution of the XPS N1s peak for nitrided carbon fibers suggested that nitriding led to the most sizeable increase in pyridinic nitrogen groups (Figure 10). Though the relative amount of amine/amide groups with respect to all nitrogen groups decreased upon nitriding in this study, the larger amount of surface nitrogen-containing groups exhibited by nitrided carbon fibers compared to natural carbon fibers suggests that the total number of amine/amide groups also increased. Liu and coworkers[43] observed that about 68% of the nitrogen atoms introduced by nitriding commercially available Printex G, a carbon black, were associated with amine/amide groups, which they expected to serve as the main attachment site for AuNPs. However, Liu et al. also found that AuNPs can deposit on pyridinic and quaternary nitrogen atoms present on the surface of nitrided carbon blacks based on their findings with AuNPs deposited from solutions with pH < 4 or > 10.

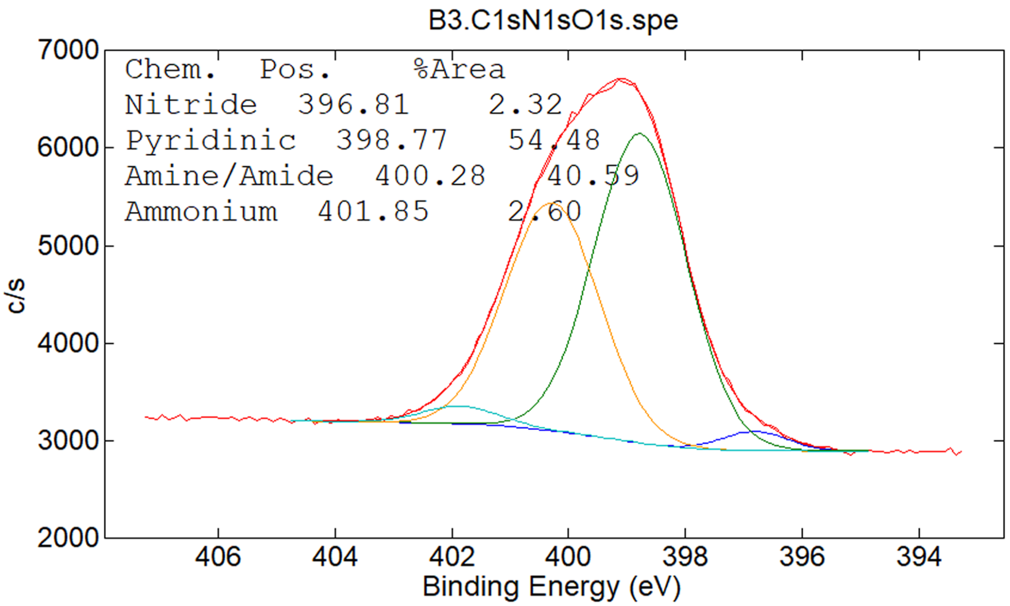

Figure 10: XPS spectra of types of nitrogen compounds present after nitriding carbon fiber

Electrochemical Characterization of Bare AuNPs Deposited on Nitrided Carbon Fiber UMEs by Direct Reduction

Upon fabrication of nitrided carbon fiber UME with the same pulling parameters as untreated carbon fiber UME, nitriding did not seem to adversely affect electrochemical response of the resulting UME. Like natural carbon fiber UMEs, nitrided carbon fiber UMEs also exhibited a sigmoidal response for the $FcCH_2OH$ / $FcCH_2OH^+$ redox couple (Figure 11). The effective radius of the electrode was estimated to be 400 nm based on the limiting current. Such small electrodes are often difficult to obtain from untreated carbon fibers due to challenges associated with electrode fabrication. The nitriding of the carbon fiber may have reduced the size of the commercially available carbon fiber hence making fabrication of smaller electrodes easier.

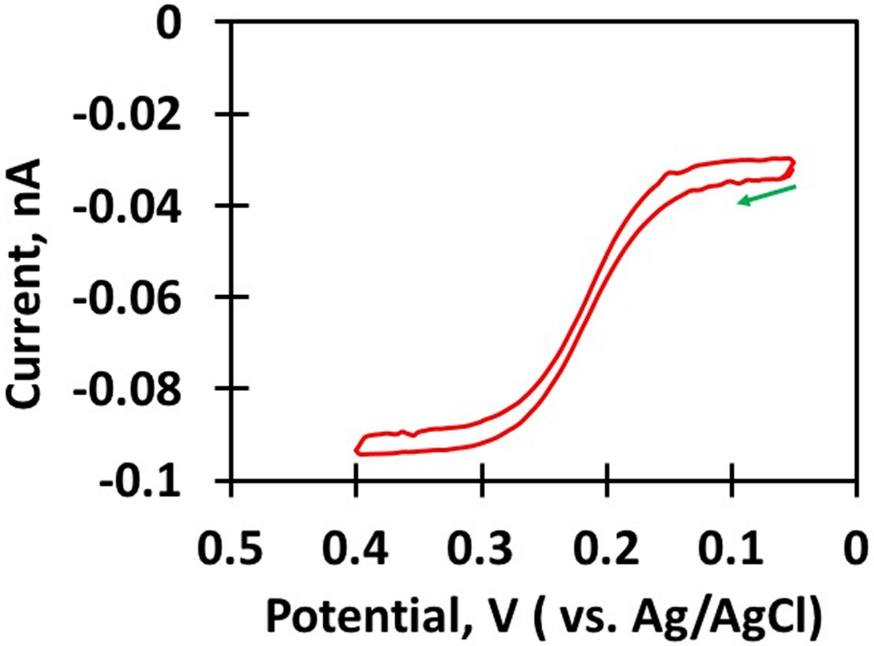

Figure 11: Representative CV of 0.50mM ferrocene methanol in 0.10M KCl with nitrided carbon fiber UME. Arrow indicates direction of scan. Scan rate of 10 mV/s.

Direct attachment of bare gold nanoparticles to the nitrided carbon fiber UME surface was carried out in the same manner as was attempted on natural carbon fiber UMEs. CVs taken in 0.50 M H_2SO_4 after deposition of bare AuNPs confirm the presence of gold (Figure 8). Though signal associated with the oxidation of gold (between +1.2 and +1.4 V vs. Ag/AgCl) was difficult to discern from the large background current at highly positive potentials, the occurrence of a cathodic peak at +0.66 V against Ag/AgCl is consistent with the reduction of gold oxide that was previously reported for bare AuNPs (6-20 nm) deposited on Pt nanoelectrodes.[40,41] While attachment of bare AuNPs on untreated carbon fiber UMEs was unsuccessful as previously mentioned (Figure 7), attachment of bare AuNPs on nitrided carbon fiber UMEs was likely made possible by the affinity enhancement associated with the increase in surface nitrogen content.

The charge correlated with the Au oxide reduction peak at +0.66 V for the AuNP modified nitrided carbon fiber UME was used to determine the surface area corresponding to the AuNP. A charge of 83.5 nC was found by integrating the peak. This corresponds to an electroactive gold surface area of 208.8 μm^2, which is ~11x larger than the surface area of AuNPs that were deposited on a much larger carbon fiber UME through LbL (Figure 5).

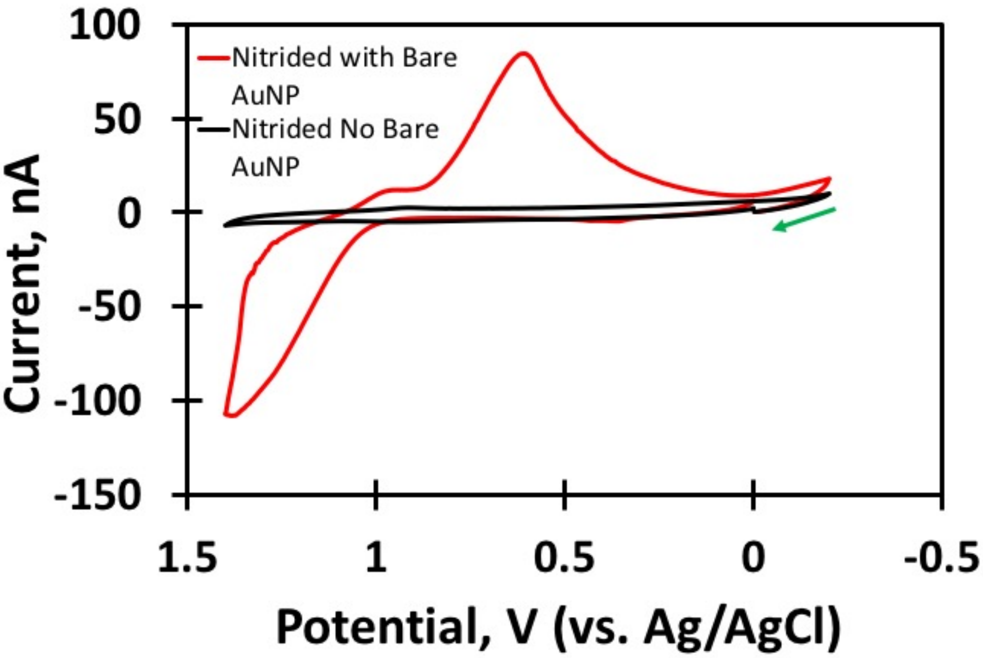

Figure 12: Representative CV responses of nitrided carbon fiber UMEs taken in 0.50 M H_2SO_4 before and after direct attachment of uncapped (bare) AuNP. Arrow indicates direction of scan. Scan rate of 100 mV/s.

CHAPTER 4

CONCLUSIONS

Studying the physical characteristics of metal nanoparticle and their effects on catalytic properties remains a crucial area of nanoparticle catalysis research that is essential for the development of efficient, cost-effective and robust catalysts. Recently, single nanoparticle electrochemical techniques have emerged to support these efforts by providing the means to investigate electrocatalytic properties in the absence of complicating factors like nanoparticle loading, interparticle distance, and heterogeneity that are present when collections of particles are studied.

In this work, methods of immobilizing gold nanoparticles on carbon ultramicroelectrodes were investigated to assess their feasibility as strategies for single nanoparticle measurements. While direct reduction of gold on electrodes prepared from commercially available PAN-based carbon fibers proved unsuccessful, similar electrodes to which GSH-AuNPs were electrostatically adsorbed through an LbL method using PDDA produced the expected redox peaks confirming the presence of gold. The charge associated with the nanoparticle coverage was used to estimate the active GHS-AuNP surface area as 18.45 μm^2. From the surface area of a single AuNP and the extent of coverage, approximately 366,000 GSH-AuNP were found to be immobilized on the natural carbon fiber UME surface.

In order to immobilize bare AuNPs on carbon ultramicroelectrodes, a soft nitriding process was carried out on carbon fibers prior to electrode fabrication. The nitriding process led to a significant increase in the intensity of N1s peak. The increase in surface nitrogen content corresponded to a ~3.5x larger atomic concentration of nitrogen compared to carbon fibers that were not nitrided. Deconvolution of the XPS N1s peak for the nitrided carbon fibers suggested that nitriding resulted in a significant increase in both pyridinic and amine/amide groups. Attaching bare AuNPs to the nitrided carbon fiber UME via the direct reduction strategy proved successful by the occurrence of characteristic oxidation and reduction peaks at +1.25 V and +0.66 V, respectively associated with the presence of gold. From the charge associated with Au oxide reduction peak for bare AuNPs immobilized on nitrided carbon fiber UME, the active gold surface area was estimated to be 208.8 μm^2, which suggests extensive surface coverage of the carbon fiber UME.

Since both layer by layer modification strategy and the nitrided carbon fiber immobilization have been proved successful, future studies will focus on fabricating nanoelectrodes with sizes similar to that of the gold nanoparticles to aid single nanoparticle immobilization on the nanoelectrode surface. The catalytic efficiencies of both capped and bare single gold nanoparticles towards methanol oxidation and other important electrocatalytic reactions will be studied. Results obtained from this study will aid in effective catalytic design and applications.

REFERENCES

1) Silvera, B.; Larson, C.A; and Kotov, N. A. Nonadditivity of nanoparticle interactions. *Science* **2015,** *350*, 1242477-1242487.

2) Link, S. M.; and A. El-Sayed A. Size and temperature dependence of the plasmon absorption of colloidal gold nanoparticles. *J. Phys. Chem.* **1999**, 103, 4212 –4217.

3) Zhou, M.; Xiao, P.; Guo, W.; Deng, J.; Liu, F.; Zhang, Y. Electrochemical synthesis of monodisperse nickel with predominant {111} orientation and high electro-oxidation activity for methanol. *J. Electrochem. Soc.* **2014,** 161, 133−137.

4) Wang, R.; He, H.; Liu, L.-C.; Dai, H.-X.; Zhao, Z. Shape-dependent catalytic activity of palladium nanocrystals for the oxidation of carbon monoxide. *Catal. Sci. Technol.* **2012,** 2, 575−580.

5) Campbell, F.W.; and Compton, R.G. The use of nanoparticles in electroanalysis: an updated review. *Anal. Bioanal. Chem.* **2010**, 396, 241 – 259.

6) Bard, A.J. Monitoring the electrochemistry of single molecules by surface-enhanced raman spectroscopy *J. Am. Chem. Soc.* **2010**, 132, 7559 – 7567.

7) Sambur, J. B.; Chen, P. Approaches to single-nanoparticle catalysis. *Annu. Rev. Phys. Chem*. **2014**, 65, 395−422.

8) Jain, P. K.; Huang, X.; El-Sayed, I. H.; and El-Sayed, M. A. Noble metals on the nanoscale: optical and photothermal properties and some applications in imaging, sensing biology, and medicine. *Acc. Chem. Res.* **2008**, 41, 1578−1586.

9) Zamborini, F. P.; Bao, L.; and Dasari, R. Nanoparticles in measurement science. *Anal. Chem.* **2012**, 84, 541−576.

10) Xiao, X.; Pan, S.; Jang, J.S.; Fan, F.R.F.; and Bard, A.J. Single nanoparticle electrocatalysis: effect of monolayers on particle and electron transfer. *J. Phys. Chem*. **2009**, 113, 14978 – 14982.

11) Campisi, S.; Schiavoni, M.; Chan-Thaw, E.; and Villa, A. Untangling the role of the capping agent in nanocatalysis: recent advances and perspectives. *Catalysts* **2016,** *6*, 185-206.

12) Shao, M.; Petes, A.; and Shoemaker, K. Electrocatalysis on platinum nanoparticles: particle size effects on oxygen reduction reaction reactivity. *Nano Lett.* **2011,** 11, 3714-3719.

13) Zhang, J.; Mo, Y.; Vukmirovic, M. B.; Klie, R.; Sasaki, K.; and Adzic, R. R. Platinum monolayer electrocatalysts for O_2 reduction: Pt monolayer on Pd (111) and on carbon-supported Pd nanoparticles. *J. Phys. Chem.* **2004,** 108, 10955-10964.

14) Mistry, H.; Reske, R.; Zheng, Z.; Zhao, Z.; Greeley, J.; Strasser, P.; and Guenya B. Exceptional size-dependent activity enhancement in the electroreduction of CO_2 over Au nanoparticles. *J. Am. Chem. Soc.* **2014,** 136, 16473-16476.

15) Mostafa, S.; Behafarid, F.; Croy, J. R.; Ono, L. K.; Li, L.; Yang, J. C.; Frenkel, A. I.; and Cuenya, R. Shape-dependent catalytic properties of Pt nanoparticles. *J. Am. Chem. Soc.* **2010,** 132, 15714-15719.

16) Higuchi, E.; Uchida, H.; and Watanabe, M. Effect of loading level in platinum-dispersed carbon black electrocatalysts on oxygen reduction activity evaluated by rotating disk electrode. *J. Electrochem. Soc***. 2005,** 583, 69-76.

17) Gamez, A.; Richard, D.; and Gallezot, P. Oxygen reduction on well-defined platinum nanoparticles inside recast ionomer. *Electrochimica. Acta.* **1996,** 41, 307-314.

18) Kumar, S.; and Zou, S. Electrooxidation of CO on uniform arrays of Au nanoparticles: effects of particle size on interparticle spacing. *Langmuir.* **2009,** 25, 574-581.

19) Spatz, J. P.; Mossmer, S.; Hartmann, C.; Moller, M.; Herzog, T.; Krieger, M.; Boyen, H. G.; Ziemann, P.; and Kabius, B. Ordered deposition of inorganic clusters from micellar block copolymer films. *Langmuir.* **2000,** 16, 407–415.

20) Taylor, S.; Fabbri, E.; Levecque, P.; Schmidt, T.; and Conrad, O. The effect of platinum loading and surface morphology on oxygen reduction activity. *Electrocatalysis.* **2016,** 7, 287-298.

21) Xu, W.; Kong, J.S.; and Chen, P. Probing the catalytic activity and heterogeneity of Au-nanoparticles at the single-molecule level. *Phys Chem Chem Phys.* **2009**, 11, 2767-2778.

22) Xiao, X.; Fan, F.-R.F.; Zhou, J.; and Bard, A.J. Current transients in single nanoparticle collision events. *J. Am. Chem. Soc*. **2008**, 130, 16669-16677.

23) Jeerage, K. M.; Candelaria, S. L.; and Stavis, S. M. Rapid synthesis and correlative measurements of electrocatalytic Nickel/Iron oxide nanoparticles. *Scientific Reports* **2018,** 8, 4584-4592.

24) Mirkin, M.; Sun, T.; Yu, Y.; and Zhou, M. Electrochemistry at one nanoparticle. *Acc. Chem. Res.* **2016,** *49,* 2328−2335.

25) Li, Y.; Cox, J. T.; and Zhang, B. Electrochemical responses and electrocatalysis at single Au nanoparticles. *J. Am. Chem. Soc.* **2010**, 132, 3047−3054.

26) Yu, Y.; Gao, Y.; Hu, K.; Blanchard, P.-Y.; Noël, J.-M.; Nareshkumar, T.; Phani, K. L.; Friedman, G.; Gogotsi, Y.; and Mirkin, M. V. Electrochemistry and electrocatalysis at single gold nanoparticles attached to carbon nanoelectrodes. *Chem Electro Chem*. **2015**, 2, 58−63.

27) Xiao, X.; and Bard, A.J. Observing single nanoparticle collisions at an ultramicroelectrode by electrocatalytic amplification. *J. Am. Chem. Soc*. **2007**, 129, 9610-9612.

28) Rees, N.V.; Zhou, Y.-G.; and Compton, R.G. Making contact: charge transfer during particle-electrode collisions. *RSC Advances*. **2012**, 2, 379-384.

29) Zhou, H.; Fan, F.-R.F.; and Bard, A.J. Observation of discrete Au nanoparticle collisions by electrocatalytic amplification using Pt ultramicroelectrode surface modification. *J Phys Chem Lett.* **2010**, 1, 2671-2674.

30) Rees, N.V.; Zhou, Y.-G.; and Compton, R.G. Making contact: charge transfer during particle-electrode collisions. *RSC Advances.* **2012,** 2, 379-384.

31) Kwon, S. J.; Fan, F.-R. F.; and Bard, A. J. Observing iridium oxide (IrOx) single nanoparticle collisions at ultramicroelectrodes. *J. Am. Chem. Soc.* **2010,** 132, 13165−13167.

32) Hodson, H.; Li, X.; Batchelor-McAulye, C.; Shao, L.; and Compton, G.C. Single nanotube voltammetry: current fluctuations are due to physical motion of the nanotube. *J. Phys. Chem. C*. **2016,** 11, 6281-6286.

33) Dasari, R.; Robinson, D. A.; Stevenson, K. J. Ultrasensitive analytical tool for detecting sizing and evaluating the catalytic activity of platinum nanoparticle. *J. Am. Chem. Soc.* **2013,** 135, 570−573.

34) Oja, S. M.; Wood, M.; and Zhang, B. Nanoscale electrochemistry. *Anal. Chem.* **2013,** 85, 473−476.

35) Oja, S.M.; Fan, Y.; Armstrong, M.C.; Defnet, P.; and Zhang, B. Nanoscale electrochemistry revisited. *Anal Chem.* **2016,** 88, 414-430.

36) Cox, J. T.; and Zhang, B. Nanoelectrodes: Recent advances and new directions. *Annu. Rev. Anal. Chem.* **2012,** 5, 253−272.

37) Yu, Y.; Gao, Y.; Hu, K.; Blanchard, P.Y.; Noel, J.M; Nareshkumar, T.; Phani, K. L.; Friedman, G.; Gogotsi, Y.; Mirkin, M. V. Electrochemistry and electrocatalysis at single gold nanoparticles attached to carbon nanoelectrodes, *Chem. Electro. Chem*. **2015,** 2, 58 – 63.

38) Yu, Y.; Noel, J. M.; Mirkin, M.V. Carbon pipette-based electrochemical nanosampler. *Anal. Chem.* **2014,** 86, 3365−3372.

39) Wang, G.; Zhang, B.; Wayment, R.J.; Harris, M.J.; and White, S.H. Electrostatic-gated transport in chemically modified glass nanopore electrodes. *J. Am Chem. Soc.* **2006,** 128, 7679-7686.

40) Sun, P.; Li, F.; Yang, C.; Sun, T.; Kady, I.; Hunt, B.; and Zhuang, J. Formation of a single gold nanoparticle on a nanometer-sized electrode and its electrochemical behaviors. *J. Phys. Chem.* **2013.** 117, 6120-6125.

41) Lakbub, J.; Pouliwe, A.; Kamasah, A.; Yang, C.; and Sun, P. Electrochemical behaviors of single gold nanoparticles. *Electroanalysis.* **2011,** 23, 2270-2274.

42) Clausmeyer, J.; Masa, J, Ventosa, E.; Ohl, D.; and Schuhman W. Nanoelectrodes reveal the electrochemistry of single nickel hydroxide nanoparticles. *Chem. Commun.* **2016,** 52, 2408-2411.

43) Lui, B.; Yao, H.; Song, W.; Jin, Lei.; Mosa, M.I.; and Rusling, J.F. Ligand free noble metal nanocluster catalysts on carbon supports via “Soft” nitriding. *J Am Chem Soc.* **2016,** 138, 4718-4721.

44) Yao, H.; Ben Liu.; Mosa, M.; Bist, I.; He, P. J.; and Rusling, P. J. F. Electrocatalytic oxidation of alcohols, tripropylamine, and DNA with ligand-free gold nanoclusters on nitrided carbon. *Chem Electro Chem* **2016,** *3*, 2100–2109.

45) P.M.A. Sherwood, "Composites" in "Handbook of surface and interface analysis - methods for problem-solving – second edition", Edited by J.C. Rivière and S. Myhra, Markel Dekker. Inc, New York, Chapter 14, in press, **2007.**

46) Mirkin, M.V. Nanoelectrodes and Liquid/Liquid Nanointerfaces. In Nanoelectrochemistry; Mirkin, M.V., Amemiya, S., Eds.; CRC Press, Boca Raton, FL, **2015,** 539-572.

47) Sutter Instrument Co. P-2000 Micropipette Puller, **2012,** 2.4, 16-7.

48) Ying, Y.; Ding, Z.; Zhan, D.; and Long Y. Advanced electroanalytical chemistry at nanoelectrodes. *Chem Sci.* **2017**, 8, 3338-3348.

49) Bishop, G.W.; Ahiadu, B.K.; Smith, J.L.; and Patterson, J.D. Use of redox probes for characterization of layer-by-layer gold nanoparticle-modified screen-printed carbon electrodes. *J. Electrochem. Soc*. **2017**, 164, 23-28.

50) Kadara, R.O.; Jenkinson, N.; and Banks, C.E. Characterization of commercially available electrochemical sensing platforms. *Sens. and Actuat. B* **2009**, 138, 556-562.

51) Chikkaveeraiah, V.B.; Mani, V.; Patel, V.; Gutkind, J.S.; and Rusling, J.F. Microfluidic electrochemical immunoarray for ultrasensitive detection of two cancer biomarker proteins in serum. *Biosens. Bioelectron*. **2011**, 26, 4477– 4483.

52) Ahiadu B. K., Role of nanoparticles in voltammetric signal enhancement exhibited by layer-by-layer (LbL) gold nanoparticle-modified screen-printed carbon electrodes (SPCEs). MS. Thesis, East Tennessee State University, Johnson City, **2017**.

53) Haiss, W.; Thanh, N.T.K.; Aveyard, J.; and Fernig, D.G. Determination of size and concentration of gold nanoparticles from UV-Vis spectra. *Anal. Chem.* **2007,** 79, 4215-4221.

54) Link, S.; and El-Sayed, M.A. Shape and size dependence of radiative, non-radiative and photothermal properties of gold nanocrystals. *Int. Rev. in Phys. Chem.* **2000,** 19, 409-453.

55) Mani, V.; Chikkaveeraiah, B.V.; Patel, V.; Gutkind, J.S.; and Rusling, J. F. Ultrasensitive immunosensor for cancer biomarker proteins using gold nanoparticle film electrodes and multienzyme-particle amplification. *ACS Nano*. **2009**, 3, 585-594.

56) Deraedt, C.; Salmon, L.; Gatard, S.; Ciganda, R.; Hernandez, Ricardo.; Ruiz, J.; and Astruc, D. Sodium borohydride stabilizes very active gold nanoparticle catalysts. *Chem. Commun.* **2014,** 50, 14194-14196.

57) Jeerage, K. M.; Candelaria, S. L.; and Stavis, S. M. Rapid synthesis and correlative measurements of electrocatalytic Nickel/Iron oxide nanoparticles. *Scientific Reports* **2018,** *8,* 4584-4594.

58) Alexeyeva, N.; and Tammeveski, K. Electroreduction of oxygen on gold nanoparticles/PDDA-MWCNT nanocomposites in acid solution. *Analytica Chimica Acta.* **2008,** 618, 140-146.

59) Trasatti, S.; and O. A, Petrii. Real Surface area measurements in electrochemistry. *Pure Appl. Chem*. **1992**, 63, 353-376.

60) Adams L, K.; Jena K, B.; Percival J, S.; and Zhang, B. Highly sensitive detection of exocytotic dopamine release using a gold-nanoparticle-network microelectrode. *Anal Chem.* **2011,** 83, 920-927.

61) Huang, X. Fabrication and properties of carbon fibers. *Materials.* **2009**, 2, 2369-2403.

62) Viswanathan, H.; Wang, Y.; Audi, A.A.; Allen, J.P.; and Sherwood M.A.P. X-ray photoelectron spectroscopic studies of carbon fiber surfaces. 24. Interfacial interactions between polyimide resin and electrochemically oxidized PAN-based carbon fibers. *Chem. Mater.* **2001,** 13, 1647-1655.

63) Smiley, J.R.; and Delgass, N.W. AFM, SEM and XPS characterization of PAN-based carbon fibers etched in oxygen plasmas. *J Mater. Sci.* **1993,** 28, 3601-3611.

VITA

GEORGE P. AFFADU-DANFUL

Education:	MS Chemistry, East Tennessee State University, Johnson City, TN, 2018. B. Sc. Chemistry, University of Cape Coast, Ghana, 2015.
Professional Experience:	Laboratory Intern, Gold Fields Ghana, Tarkwa, Ghana (June - July 2012).
	Laboratory Intern, Ghana Water Company Limited, Accra, Ghana (June - July 2013).
	Teaching Assistant, University of Cape Coast, Ghana, (2015 - 2016).
	Graduate Teaching Assistant, East Tennessee State University, Johnson City, TN (2016 - 2018).
	Research Assistant, (Dr. Gregory Bishop's Research Lab), East Tennessee State University, Johnson City, TN (2018).
Research Experience:	Graduate research student, East Tennessee State University, Johnson City, TN (2016 - 2018) (Mentor: Dr. Gregory Bishop)
	Fabricated gold and carbon fiber Ultramicro and nanoelectrodes and characterized them.
	Synthesized bare and glutathione capped gold nanoparticles.
	Conducted electrochemical measurements.
	Undergraduate research student, University of Cape Coast, Ghana, (2014 - 2015) (Mentor Dr. Francis Nsiah)
	Synthesized silver nanoparticles
	Prepared activated carbon packed column to purify groundwater.

Presentations:

Theophilus Neequaye, George P. Affadu-Danful,
Gregory W. Bishop.
Preparation and Characterization of Carbon Fiber Ultramicroelectrodes for Electrocatalytic Studies of Single Gold Nanoparticles, 69th South East Regional Meeting of the American Chemical Society, Charlotte, NC., 2017,
(11/09/2017, Poster Presentation, SERMACS 201366).

George P. Affadu-Danful, Theophilus Neequaye,
and Gregory W. Bishop.
Immobilization of Gold Nanoparticles by Direct Reduction on Nitrided Carbon Fiber Ultramicroelectrodes as a platform for Measuring Electrocatalytic Properties,
2018 Appalachian Student Research Forum,
East Tennessee State University, Johnson City, TN
(05/05/2018, Oral Presentation, ASRF 2018).

George P. Affadu-Danful, Theophilus Neequaye,
and Gregory W. Bishop.
Immobilization of Bare Gold Nanoparticles by Direct Reduction on Nitrided Carbon Fiber Ultramicroelectrodes as a platform for Measuring Electrocatalytic Properties, Graduate Seminar,
East Tennessee State University, Johnson City, TN
(05/06/2018, Oral Presentation, ASRF 2018).

Honors and Awards:

First Place in Master's Natural Science Group A Oral Presentation,
Appalachian Student Research Forum 2018,
East Tennessee State University, Johnson City, TN